POTENTIAL OF SMALL-SCALE TURBOMACHINERY FOR WASTE HEAT RECOVERY ON AUTOMOTIVE INTERNAL COMBUSTION ENGINGES

Kévin ROSSET[1*], Violette MOUNIER[1], Eliott GUENAT[1], Olivier PAJOT[2], Jürg SCHIFFMANN[1]

[1]Ecole Polytechnique Fédérale de Lausanne, Laboratory for Applied Mechanical Design, Neuchâtel, Switzerland
kevin.rosset@epfl.ch, violette.mounier@epfl.ch, eliott.guenat@epfl.ch, jurg.schiffmann@epfl.ch

[2]PSA Peugeot Citroën, Research, Innovation & Advanced Technologies Division, Lausanne, Switzerland
olivier.pajot@mpsa.com

* Corresponding Author

ABSTRACT

This paper investigates the waste heat recovery potential of internal combustion engines, using organic Rankine cycles running on small-scale radial turbomachinery. ORC are promising candidates for low-grade thermal sources and the use of dynamic expanders yields very compact systems, which is advantageous for automotive applications. As engine coolant and exhaust gases are the major available heat sources, different cycle configurations and working fluids have been investigated to capture them, in both urban and highway car operation. Pareto fronts showing the compromise between net power output and total heat exchange area have been identified for a set of cycle's variables including turbine inlet conditions and heat exchanger pinches. A preliminary optimization, including only R-1234yf working fluid, shows that a single-source regenerative cycle harvesting the high temperature exhaust gas stream performs averagely better than coolant-driven and dual-source cycles. A more in-depth optimization including eight working fluids as well as aerodynamic and conceptual limitations related to radial turbomachinery and automotive design constraints, finally shows that an ICE exhaust heat recovery ORC could improve the first law efficiency of the driving system by up to 10% when implemented with fluid R-1233zd.

1. INTRODUCTION

Nowadays, concerns about fossil fuel shortage and global warming advocate for a more rational use of primary energy. Transportation, which represents about 28% of the world energy consumption (IEA, 2014), is a sector where efficiency improvements are particularly awaited. Indeed, according to Legros (2014) passenger cars are barely using one third of the available fuel power to drive the wheels. The remaining two thirds are rejected to the environment as waste heat, mainly through coolant and exhaust gas streams. Recovering part of this energy would not only save fuel but also decrease pollutants emissions. The conversion of heat into useful electrical or mechanical energy may be performed by technologies like thermoelectric, thermoacoustic and thermophotovoltaic generators or by various thermodynamic cycles such as Stirling, Brayton and Rankine cycles, according to Legros (2014). Although they are compact, thermoelectric devices require expensive materials and have rather low efficiency, as shown by LeBlanc (2014). As it can be seen in Wu *et al.* (2014) ongoing research on thermoacoustic generators shows good efficiency but prototypes are still bulky. Thermophotovoltaic systems are getting mature but prototypes show limited efficiency and mostly, they require a high temperature source, involving combustion, to efficiently convert heat into thermal radiations (Ferrari *et al.* 2014). Although free-piston Stirling engines are an efficient and mature

technology, they are best suited to slow changing of power output and require long warm-up period (Kongtragool and Wongwises 2003). While open Brayton cycles are adequately exploited in gas turbines and turbojet engines, their efficiency seriously drops when trying to operate them in closed loop with a low temperature heat source. To compensate for this, Wright *et al.* (2006) proposed a design with multiple inter-stage heating/cooling between the expansion/compression stages. The resulting complexity and associated cost make this cycle unsuitable for vehicle integration. Rankine cycles are an attractive candidate, especially when running with organic working fluids, where low- to medium-grade heat sources can be harvested, as shown in the review by Sprouse and Depcik (2013). In such systems, the expansion technology is the most important element since it is responsible for the extraction of the fluid power. For small-scale power generation, volumetric expanders are usually selected since they can handle low fluid flowrates. However, friction between the moving parts causes wear and eventually failure if no lubricant is mixed with the working fluid. In addition to reducing expander and evaporator performance, auxiliary oil circuits add complexity and cost to the system. For these reasons, dynamic expanders would be the preferred solution. In the turbomachinery domain, radial inflow turbines are promising since they can achieve much higher stage pressure ratios than axial machines. Yet, in order to process low flowrates, radial rotors need to be downsized, which is advantageous for vehicle packaging, but however implies high rotor speeds. Improvements in dynamic gas bearing technology make this possible, as shown by Schiffmann and Favrat (2009) and Demierre *et al*. (2015), who successfully operated small-scale radial turbo-compressors and turbo-expanders at speeds up to 210 krpm. The objective of this article is to evaluate the potential of Rankine cycles combined with small-scale turbomachines for waste heat recovery on automotive internal combustion engines. Several cycle topologies and working fluids are included in the investigation to identify the most promising configuration for maximizing waste heat recovery while reducing the required heat exchange area.

2. SYSTEM DESCRIPTION

2.1 Engine characterization

The considered commercial vehicle is equipped with a 96 kW gasoline engine. Test data have been analyzed to extract waste heat flows and temperatures associated with urban (50 km/h) and highway (120 km/h) operations. As shown in Table 1, exhaust gas and coolant streams were identified as valuable heat sources with respect to the engine power. From an exergetic point of view though, coolant yields significantly less recoverable power than exhaust gases, due to its lower temperature.

Table 1: Vehicle power streams characterized in terms of temperature, power and exergy

Vehicle operating point	Engine	Exhaust gases			Coolant			
	$\dot{W}_{mec}$	T	$\dot{Q}$	$\dot{E}$	T_{in}	T_{out}	$\dot{Q}$	$\dot{E}$
	kW	°C	kW	kW	°C	°C	kW	kW
Urban	3.80	425	2.64	0.97	105	104	2.17	0.46
Highway	22.9	706	19.2	9.21	105	101	12.6	2.61

2.2 Cycle configurations

In order to extract useful power from engine waste heat, a basic Rankine cycle (Figure 1a) is first considered. In this cycle, a selected working fluid is successively compressed through a pump where little power is consumed (1-2), evaporated through a heat exchanger in contact with a heat source (2-3), expanded through a turbine where useful power is extracted (3-4), and finally condensed through a heat exchanger in contact with a heat sink (4-1) considered to be ambient air in the studied system. To further increase the cycle efficiency, an internal heat exchanger (IHX) can be added as shown in Figure 1b, so that the working fluid is preheated (resp. precooled) before being evaporated (resp. condensed). Yet, in these two configurations, only one single source can be harvested. Since the goal is to maximize heat recovery, two additional configurations are proposed, where both the exhaust gas

and the coolant heat sources are exploited. The first one uses two heat exchangers in series (Figure 1c), with the coolant stream preheating the working fluid and the exhaust gas stream evaporating it. The second one integrates two pumping and expansion stages with heat exchangers in parallel (Figure 1d). In this configuration, the coolant and exhaust gas streams are respectively associated with the intermediate and high pressure evaporators. Although other configurations could have been studied, it was decided, in view of the targeted automotive application where compact packaging is a key aspect, to limit the number of heat exchangers in the evaluated systems to a maximum of three. In order to reduce exergetic losses, all evaporators are considered counter-flow and all condensers cross-flow. The first type is well suited to transfer heat from the engine waste heat streams to the working fluid while the second one is better adapted to reject heat from the working fluid to the ambient air.

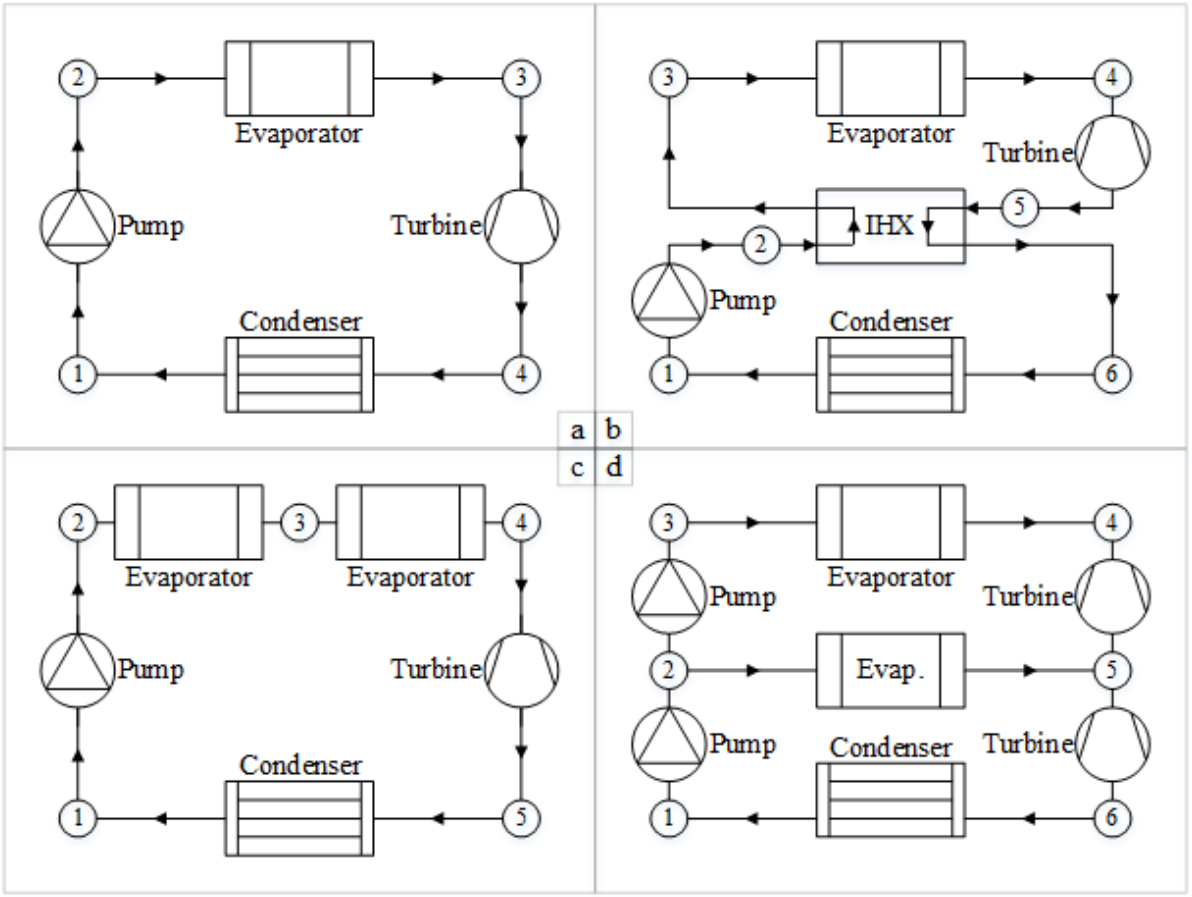

Figure 1: Evaluated Rankine cycle configurations: Basic single-source (a), Regenerative single-source (b), Series dual-source (c), Parallel dual-source (d)

2.3 Fluid candidates

Several working fluids may be appropriate candidates for Rankine cycles. Beyond the critical point, indicating the maximum pressure and temperature levels at which a fluid can experience a two-phase state, environmental indicators are also essential selection criteria. As such, working fluids should show null Ozone Depletion Potential (ODP), low Global Warming Potential (GWP) and low toxicity and flammability (ASHRAE standard 34). Refrigerants R-134a, R-152a and R-245fa were consequently identified as good candidates. Because of their high GWP however, R-134a and R-245fa are likely to be phased out and replaced by their respective counterparts R-1234yf/R-1234ze and R-1233zd, which are therefore included in the evaluation. Other considered fluids are ethanol and water. Table 2 summarizes the selected fluids, also highlighting their expansion behavior from a saturated vapor state at the turbine inlet.

Rankine cycles generally operate close to the saturation lines. Therefore ideal or perfect gas assumptions to retrieve the fluid's thermodynamic properties are not valid. This article uses REFPROP® based thermodynamic data to perform cycle calculations.

Table 2: Working fluid candidates

Working fluid	P_{cr} [bar]	T_{cr} [°C]	ODP	GWP	ASHRAE 34	Expansion
R-134a	40.6	101	0	1430	A1	Wet
R-1234yf	33.8	95	0	4	A2L	Dry
R-1234ze	36.3	109	0	6	A2L	Dry
R-152a	45.2	113	0	124	A2	Wet
R-245fa	36.5	154	0	1030	B1	Dry
R-1233zd	35.7	166	0	7	A1	Dry
Ethanol	62.7	242	0	0	-	Wet
Water	220.6	374	0	0	A1	Wet

2.4 Heat sink

In addition to the available heat sources, proposed cycle configurations, and working fluids, a heat sink also has to be characterized. As ambient temperatures ranging from 20 to 25°C were observed in the vehicle test data, the reference cold source temperature is set to 25°C. Assuming a 10°C temperature increase in the cross-flow condensers, an average air exchange temperature of 30°C is then considered.

3. SIMULATION MODELS

In order to assess the performance of a Rankine cycle on the two vehicle operating points, steady-state models have been implemented for each cycle configuration. Typical model inputs are the heat source and sink mass flowrates and temperatures, working fluid subcooling/superheating at the pump/turbine inlets, turbomachines efficiency and heat exchangers temperature pinch. Calculated outputs are the system efficiency, net power output, turbomachinery pre-design (rotor speed and diameter) and heat exchangers area. Model resolution is based on mass and energy conservation laws with the following general assumptions:

- Fluid flow is one-dimensional.
- Fluid kinetic and potential energy variations are neglected.
- Heating and cooling transformations are isobaric.
- Heat exchangers are perfectly insulated.

3.1 Turbomachinery modeling

The net power output of a cycle is calculated from the difference of the generated turbine powers $\dot{W}_t$ and consumed pump powers $\dot{W}_p$. Each of them is predicted from the product of the working fluid mass flowrate ($\dot{m}_t$, $\dot{m}_p$) with the isentropic specific enthalpy difference through the device ($\Delta h_{t,s}$, $\Delta h_{p,s}$), corrected to account for entropy and electromechanical losses:

$$\dot{W}_{net} = \sum_t \dot{W}_t - \sum_p \dot{W}_p = \sum_t \left(\dot{m}_t \Delta h_{t,s} \cdot \eta_{t,s}\eta_{t,em}\right) - \sum_p \left(\dot{m}_p \Delta h_{p,s} / \eta_{p,s}\eta_{p,em}\right) \qquad (1)$$

While electromechanical efficiencies $\eta_{t/p,em}$ are considered fixed for simplicity, isentropic efficiencies $\eta_{t/p,s}$ are extracted from Balje's diagrams (Balje, 1981), that plot iso-efficiency lines as a function of specific speed n_s and specific diameter d_s, defined as:

$$n_s = \frac{\omega \, \dot{V}^{0.5}}{|\Delta h_s|^{0.75}} \tag{2}$$

$$d_s = \frac{d \, |\Delta h_s|^{0.25}}{\dot{V}^{0.5}} \tag{3}$$

Determining these two dimensionless parameters from the optimal efficiency on the radial pump / turbine diagram and knowing the fluid flowrate $\dot{V}$ at the pump inlet / turbine outlet as well as the absolute fluid isentropic enthalpy difference $|\Delta h_s|$, both the rotor angular velocity ω and tip diameter d can be estimated. Also, to avoid restricting the feasible design, radial pumps and turbines are not considered coupled on the same shaft.

3.2 Heat exchangers modeling

Predicting the volume of a heat exchanger is a difficult task. It depends not only on the flow conditions, but also on the detailed heat exchanger geometry and materials. Since heat exchangers design is beyond the scope of this work, it was decided to evaluate their size in terms of heat exchange surface. For this purpose, the Logarithmic Mean Temperature Difference (LMTD) method (Incropera *et al.*, 2006) was used. It states that the power $\dot{Q}$ exchanged between two streams is equal to:

$$\dot{Q} = UA\Delta T_{lm} \tag{4}$$

where U is the overall heat transfer coefficient, A the heat exchange area and ΔT_{lm} the logarithmic mean temperature difference. By assuming that fluids are separated by an infinitely thin wall, the heat exchange area becomes identical on each side and the overall heat transfer coefficient derives from an inverted sum of the hot and cold fluid convective heat transfer coefficients U_h and U_c; which used values are presented in Table 3, depending on the fluid type:

$$\frac{1}{U} = \frac{1}{U_h} + \frac{1}{U_c} \tag{5}$$

Table 3: Typical convective heat transfer coefficients (Marechal, 2012)

	Gas	Liquid	Condensing fluid	Evaporating fluid
U_{conv} $[W/m^2K]$	60	560	1600	3600

The LMTD is given by:

$$\Delta T_{lm} = \frac{\Delta T_2 - \Delta T_1}{\log(\Delta T_2 / \Delta T_1)} \tag{6}$$

where ΔT_1 and ΔT_2 are the fluid temperature differences between the two streams on each side of the heat exchanger.

4. OPTIMIZATION RESULTS AND DISCUSSION

The implemented models being highly non-linear, non-differentiable and with numerous inputs, a genetic algorithm has been used to perform the optimizations. The goal is to identify the most promising cycle configuration and working fluid and to determine the possible trade-offs between system performance and size, in accordance with vehicle expectations. Two objective functions were defined: net power output maximization and total heat exchange area minimization. As observed by

Molyneaux (2002) and Leyland (2002), genetic algorithms are well indicated to come up with Pareto frontiers when dealing with complex energy systems.
The optimization was performed in two stages: a first run comparing the four cycles presented in Figure 1 and a second run confronting the eight fluids listed in Table 2.

4.1 Optimization stage I

The first optimization stage aimed at comparing the cycle configurations exposed in Figure 1. It has been performed using refrigerant R-1234yf, which is the standard working fluid replacing R-134a in vehicle cabin air conditioning, with a pump inlet subcooling of 2°C, a pinch of 10°C in all heat exchangers, and no electromechanical losses. Three decision variables were accounted for, as shown in Table 4.

Table 4: Decision variables for optimization stage I

#	Decision variable	Range
1	Working fluid evaporating pressure	2 – 40 bar
2	Working fluid temperature at turbine inlet	60 – 250 °C
3	Exhaust gas temperature at evaporator outlet	80 – 200 °C

Figure 2 presents the Pareto fronts resulting from the first-stage optimization. At first glance, it can be seen that cycles recovering the coolant waste heat only are the least profitable ones and that an internal heat exchanger (IHX) does not increase the extracted power. On the contrary, single-source waste heat recovery using the exhaust gases is much more valuable and, in this case, regeneration through an IHX significantly increases the conversion to useful power. With equal powers for lower areas, the dual-source series configuration always shows better performance than the parallel configuration. This is due to the engine coolant temperature (about 100°C), which imposes the cycle intermediate pressure level (about 30 bar for R-1234yf at 90°C) and therefore limits the topping cycle pressure ratio (1.33 for a maximum pressure of 40 bar) in the parallel configuration.

In urban vehicle operation, the overall Pareto front is shared by the exhaust-gas-driven basic cycle up to 0.13 kW (36% of available power range), the exhaust-gas-driven regenerative cycle from 0.13 to 0.28 kW (42%) and finally the dual-source series cycle from 0.28 to 0.36 kW (22%). In highway vehicle operation however, only exhaust-gas-driven cycles take part in the overall Pareto front, with the basic configuration being optimal up to 1.4 kW (50% of available power range) and the regenerative configuration being optimal from 1.4 to 2.8 kW (50%). Consequently, recovering the engine exhaust gases waste heat using a Rankine cycle that includes an internal heat exchanger, gives the best vehicle efficiency improvement perspectives.

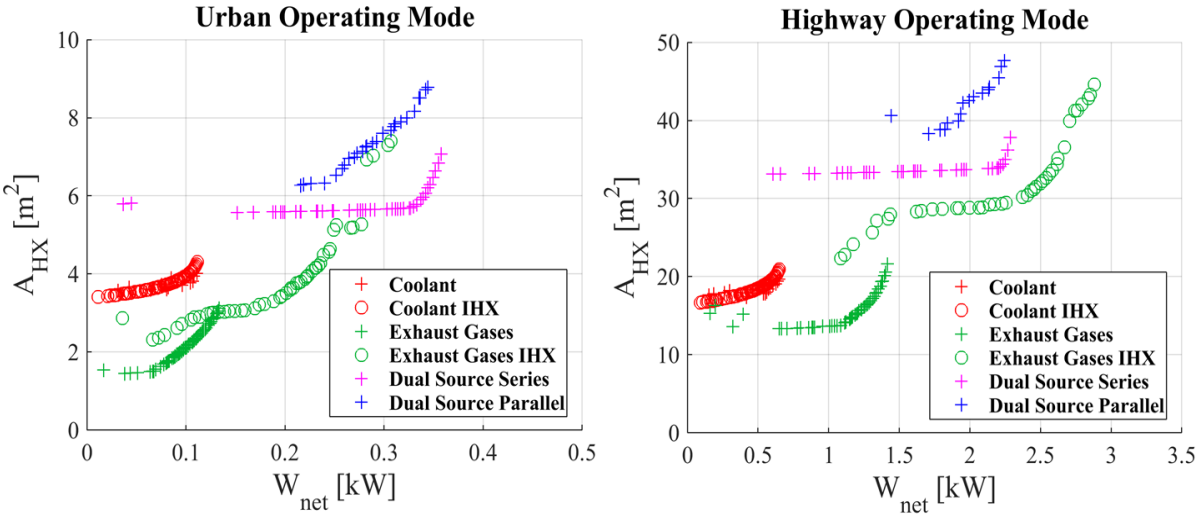

Figure 2 : Heat recovery system Pareto fronts from different cycle configurations

4.2 Optimization stage II

The second optimization stage aimed at comparing the fluid candidates exposed in Table 2. It has been performed using a regenerative exhaust-gas-driven cycle, which is the optimal configuration from the first-stage optimization, with a pump inlet subcooling of 5°C to prevent cavitation, turbomachine electromechanical efficiencies of 85% to account for bearing and generator losses, a minimum working fluid pressure of 1 bar to avoid subatmospheric processes and possible contamination by air, a maximum working fluid pressure of 30 bar to make piping and evaporator costs accessible to automotive industry, a minimum exhaust gas outlet temperature of 150°C to avoid acid condensation in the last section of the exhaust pipe, and a minimum turbine tip diameter of 10 mm for manufacturability. Furthermore, Balje's (1981) predictions for radial pump isentropic efficiencies being overestimated (up to 92%), the pump isentropic efficiency has been fixed to a more realistic value of 60%. Four decision variables were accounted for, as shown in Table 5.

Table 5: Decision variables for optimization stage II

#	Decision variable	Range
1	Working fluid superheating at turbine inlet	0 – 200 °C
2	Condenser pinch	5 – 25 °C
3	Evaporator pinch	5 – 25 °C
4	IHX pinch	5 – 25 °C

In addition to the above constraints, cycle pressure ratio limitations have been considered, so that the expansion is feasible across a single-stage turbine. The advantage is that it significantly decreases the complexity and consequently the manufacturing cost of the turbo-generator unit. Yet, as dynamic machine stage pressure ratio is strongly dependent on rotor design and fluid density differentials, a one-dimensional aerodynamic analysis has been performed on an existing small-scale radial turbine design presented by Demierre *et al.* (2015), which goal was to determine for each working fluid, the maximum stage pressure ratio as a function of the turbine inlet superheating. In this analysis, sonic limitations at the nozzle and rotor throats were accounted for, as well as a maximum rotor peripheral speed of 400 m/s, for mechanical strength reasons.

Results from the second-stage optimization (Figure 3) suggest that whether the vehicle is operated in urban or highway mode, ethanol as well as refrigerants R-245fa and its substitute clearly show the best objectives combinations, with R-1233zd being optimal in terms of net power output. Nonetheless, if the main criterion is to minimize the heat exchange area, ethanol then takes the first place in the ranking. For further comparison, Table 6 presents for each working fluid, some of the main system characteristics at maximum net power output; that is turbine diameter d_t and rotational speed N_t, cycle pressure ratio π, evaporating pressure P_{ev} and efficiency η_C, and system overall efficiency η_S. The first-law efficiencies are defined below, as a function of evaporator load $\dot{Q}_{ev}$ and heat source available power $\dot{Q}_{source}$.

$$\eta_C = \frac{\dot{W}_{net}}{\dot{Q}_{ev}} \tag{7}$$

$$\eta_S = \frac{\dot{W}_{net}}{\dot{Q}_{source}} \tag{8}$$

It should here be mentioned that the cycle condensing pressures were determined from the average heat sink temperature and accounting for the condenser pinch, subcooling at the pump inlet and minimum pressure constraint. Then, the evaporating pressure was calculated from the optimal pressure ratio at corresponding turbine inlet superheating and accounting for the maximum pressure constraint. As shown in Table 6, this last constraint mainly explains why refrigerants R-152a, R-134a and substitutes exhibit lower performance. On the contrary, with a condensing pressure of 1 bar,

natural working fluids do not suffer from the maximum pressure constraint. While water-based systems performance is limited by the zero-droplet tolerance and by the limitation of the rotor peripheral speed, ethanol-based systems show promising results with the best Pareto frontier from 0.15 to 0.2 kW in urban operating mode and from 1.5 to 1.8 kW in highway operating mode. Nonetheless, these two fluids present relatively high and therefore challenging rotational speeds (300 to 600 krpm), which associated with 20 to 10 mm rotors, lead to much higher peripheral speeds compared to refrigerant-based systems.

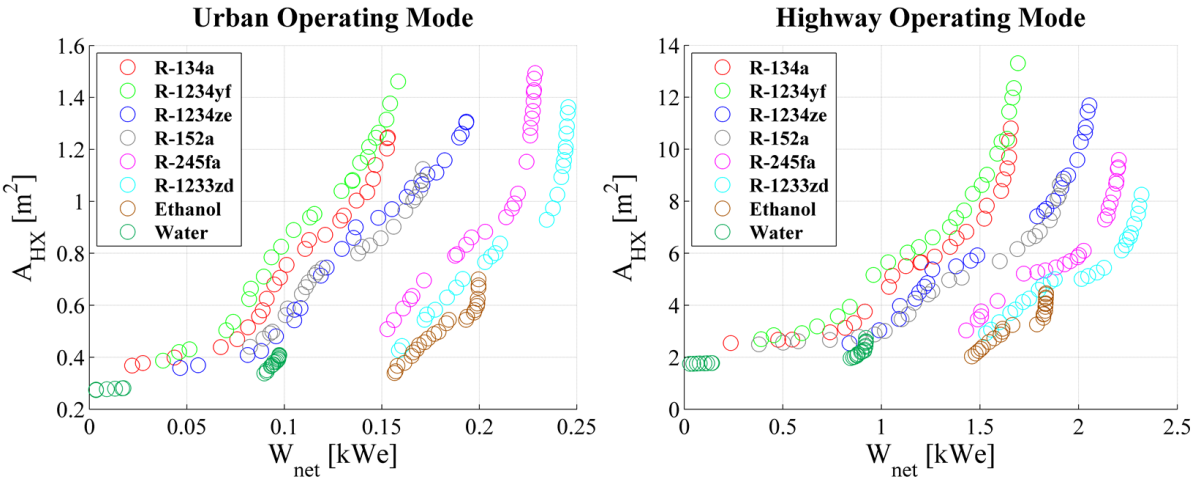

Figure 3: Heat recovery system Pareto fronts from different working fluid candidates

No matter the working fluid, turbine design is always characterized by the smallest accepted design diameter and a high rotational speed when optimizing the heat recovery system for an urban vehicle operation. This is disadvantageous for production and performance since manufacturing tolerances (linked with efficiency) and rotor balancing (linked with stability) become stricter, as observed by Schiffmann and Favrat (2010) and Schiffmann (2013). In addition, efficiencies are lower compared to the highway operation systems. Hence, from this refined optimization and considering both cycle net power outputs and turbine design characteristics, it can be concluded that the waste heat recovery system should be designed for the highway vehicle operation, using refrigerant R-1233zd as cycle working fluid. The expected gain ranges from 1.5 to 2.3 kW of electrical power that is a 6.5 to 10% increase in the first-law efficiency of the vehicle drivetrain.

Table 6: System characteristics at maximum net power outputs

	Urban						Highway					
Working fluid	η_S %	η_C %	P_{ev} bar	π -	N_t krpm	d_t mm	η_S %	η_C %	P_{ev} bar	π -	N_t krpm	d_t mm
R-134a	5.8	8.4	30.0	2.93	261	10.0	8.6	10.5	30.0	2.90	244	12.0
R-1234yf	6.0	8.7	30.0	2.94	250	10.0	8.8	10.8	30.0	2.93	214	12.9
R-1234ze	7.3	10.6	30.0	3.89	293	10.0	10.7	13.1	30.0	3.89	250	13.0
R-152a	6.5	9.4	30.0	3.20	340	10.0	10.0	12.2	30.0	3.27	368	10.9
R-245fa	8.7	12.6	18.2	5.15	309	10.0	11.4	14.0	23.6	5.18	227	15.2
R-1233zd	9.3	13.5	17.4	5.28	329	10.0	12.0	14.7	20.3	5.31	218	16.4
Ethanol	7.6	11.0	5.95	5.95	606	10.0	9.5	11.7	5.94	5.94	335	19.3
Water	3.7	5.4	2.49	2.49	600	10.4	4.8	5.9	2.49	2.49	395	17.9

5. CONCLUSIONS

In view of reducing vehicle fuel consumption and carbon dioxide emissions, Rankine cycle systems have been studied to recover the waste heat from engine coolant and exhaust gas streams. Two representative vehicle operating points were analyzed with four possible cycle configurations and a set of eight working fluids. Targeting both maximum performance and minimum size criteria, multi-objective optimizations were performed, accounting for automotive and turbomachinery design constraints. From the resulting Pareto fronts, it has been found that the optimal recovery system should be designed for the highway vehicle operation, using a regenerative exhaust-gas-driven cycle and refrigerant R-1233zd. The expected benefit is an additional 2.3 kW of electrical power that is a 10% increase in the vehicle efficiency. For achieving this performance, the optimal expander is a 16.5 mm tip diameter radial inflow turbine rotating at about 220 krpm. In order to validate the complete system design, its behavior should now be evaluated for other vehicle operating points, including off-design performance evaluation and engine dynamics.

NOMENCLATURE

Symbols

A	Area	m^2
d	Tip diameter	mm
d_s	Specific diameter	$-$
$\dot{E}$	Exergy	W
h	Specific enthalpy	J/kg
$\dot{m}$	Mass flowrate	kg/s
N	Rotational speed	rpm
n_s	Specific speed	$-$
P	Pressure	bar
$\dot{Q}$	Heat	W
T	Temperature	$°C$
U	Heat transfer coefficient	W/m^2K
$\dot{V}$	Volumetric flowrate	m^3/s
$\dot{W}$	Electrical power	We
$\dot{W}$	Mechanical power	W
Δh	Specific enthalpy diff.	J/kg
ΔT	Temperature difference	$°C$
η	Efficiency	$-$
π	Pressure ratio	$-$
ω	Angular velocity	rad/s

Subscripts

C	Cycle
c	Cold
$conv$	Convective
cr	Critical state
em	Electromechanical
ev	Evaporation
HX	Heat exchange
h	Hot
in	Inlet
lm	Logarithmic mean
mec	Mechanical
net	Net
out	Outlet
p	Pump
ref	Reference (Ambient)
S	System
s	Isentropic
t	Turbine

Acronyms

GWP	Global Warming Potential
ICE	Internal Combustion Engine
IHX	Internal Heat Exchanger
ODP	Ozone Depletion Potential
ORC	Organic Rankine Cycle

REFERENCES

Balje, O. E., 1981, *Turbomachines: A Guide to Design, Selection, and Theory*, John Wiley & Sons Inc., New York, 513 p.

Demierre, J., Rubino, A., Schiffmann, J., 2015, Modeling and Experimental Investigation of an Oil-Free Microcompressor-Turbine Unit for an Organic Rankine Cycle Driven Heat Pump, *Journal of Engineering for Gas Turbines and Power (ASME)*, vol. 137, no. 3: p. 032602.

Ferrari, C., Melino, F., Pinelli, M., Spina, P. R., 2014, Thermophotovoltaic energy conversion: Analytical aspects, prototypes and experiences, *Appl. Energy*, vol. 113: p. 1717-1730.

IEA, 2014, 2014 Key World Energy STATISTICS, *International Energy Agency*.

Incropera, F. P., DeWitt, D. P., Bergman, T. L., Lavine, A. S., 2007, *Fundamentals of Heat and Mass Transfer*, John Wiley & Sons Inc., New York, 997 p.

Kongtragool, B., Wongwises, S., 2003, A review of solar-powered Stirling engines and low temperature differential Stirling engines, *Renew. Sustain. Energy Rev.*, vol. 7: p. 131-154.

LeBlanc, S., 2014, Thermoelectric generators: Linking material properties and systems engineering for waste heat recovery applications, *Sustainable Materials and Technologies*, vol. 1-2: p. 26-35.

Legros, A., Guillaume, L., Diny, M., Zaïdi, H., Lemort, V., 2014, Comparison and Impact of Waste Heat Recovery Technologies on Passenger Car Fuel Consumption in a Normalized Driving Cycle, *Energies*, vol. 7: p. 5273-5290.

Leyland, G. B., 2002, Multi-Objective Optimization Applied to Industrial Energy Problems, *Ecole Polytechnique Fédérale de Lausanne*, PhD Thesis no. 2572.

Marechal, F., 2012, *Process integration techniques for improving the energy efficiency of industrial processes*, EPFL Advanced Energetics coursebook.

Molyneaux, A., 2002, A Pratical Evolutionary Method for The Multi-Objective Optimisation of Complex Integrated Energy Systems Including Vehicle Drivetrains, *Ecole Polytechnique Fédérale de Lausanne*, PhD Thesis no. 2636.

Schiffmann, J., Favrat, D., 2009, Experimental investigation of a direct driven radial compressor for domestic heat pumps, *Int. J. Refrig.*, vol. 32, no. 8: p. 1918-1928.

Schiffmann, J., Favrat, D., 2010 Integrated Design and Optimization of Gas Bearing Supported Rotors, *Journal of Mechanical Design*, vol. 132

Schiffmann, J., 2013 Enhanced Groove Geometry for Herringbone Grooved Journal Bearings, *Journal Of Engineering For Gas Turbines And Power (ASME)*, vol. 135, no. 10, p. 102501.

Sprouse III, C., Depcik, C., 2013, Review of organic Rankine cycles for internal combustion engine exhaust waste heat recovery, *Appl. Therm. Eng.*, vol. 51, no. 1-2: p. 711-722.

Wright, S. A., Vernon, M. E., Pickard, P. S., 2006, Concept Design for a High Temperature Helium Brayton Cycle with Interstage Heating and Cooling, *Sandia National Laboratories*.

Wu, Z., Zhang, L., Dai, W., Luo, E., 2014, Investigation on a 1kW traveling-wave thermoacoustic electrical generator, *Appl. Energy*, vol. 124: p. 140-147.